ACS Biomaterials SCIENCE & ENGINEERING
Cite This: ACS Biomater. Sci. Eng. 2019, 5, 3944−3953
Article
pubs.acs.org/journal/abseba

Remnant Effects of Culture Density on Cell Chirality After Reseeding

Hoi Kwan Kwong,[†] Yaozhun Huang,[†] Yuanye Bao,[†] Miu Ling Lam,[‡,#] and Ting-Hsuan Chen*[,†,#,§]

[†]Department of Biomedical Engineering and [‡]School of Creative Media, City University of Hong Kong, 83 Tat Chee Avenue, Hong Kong Special Administrative Region, China

[#]CityU Shenzhen Research Institute, Shenzhen 518057, China

[§]State Key Laboratory of Molecular Engineering of Polymers, Fudan University, Shanghai 200086, China

Supporting Information

ABSTRACT: Proper muscle function requires specific orientation of myotubes. Cell chirality, a mechanical behavior of cells, may participate in myogenesis and give rise to left−right (LR) orientation of muscle tissue. Thus, it is essential to understand the factors effecting the cell chirality. Here, using C2C12 cells as a model system, we report that prior culture condition with high/low density can create remnant effects on cell chirality after reseeding. C2C12 myoblasts were first conditioned by a series of subcultures with plating density at 2200 cells/cm^2 (low density) or 22 000 cells/cm^2 (high density). After reseeding on micropatterned stripes fabricated on glass or polydimethylsiloxane (PDMS) substrates, we found that the cells after low-density cultures exhibited a reduced cell aspect ratio and intercellular alignment, leading to an attenuated chiral orientation only appearing on glass substrate. In contrast, chiral orientation was observed in cells after high-density culture on both substrates. By comparing it to the original cells without being subcultured with high/low density, we found that the series of low-density cultures disorganized the formation of actin rings in single cells, which is an essential structure for cell chirality. Moreover, by using high-density culture supplemented with inhibitors of actin polymerization, the effect of low-density cultures was recaptured, suggesting that the series of subcultures with high/low density may be an in vitro aging process that modifies the actin cytoskeleton, causing a remnant attenuation of cell chirality even after trypsin digestion and reseeding. Together, our result suggests a mechanistic insight of how cytoskeletal structures "memorize" the previous experience through modification of the actin filament, opening up new possibilities for morphogenesis and mechanobiology.

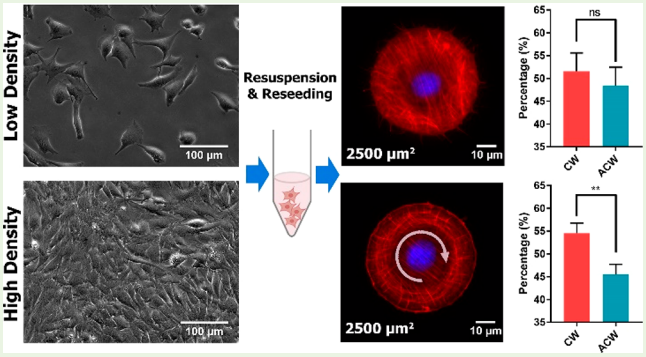

KEYWORDS: *cell density, micropatterning, left−right asymmetry, cell chirality, cell orientation*

INTRODUCTION

Skeletal muscle tissue in human body is responsible for many biological activities including prehension and locomotion. Failure of muscular functions such as traumatic injury or malignant tumor extraction may require therapeutic or cosmetic surgery.[1] Thus, it is of vital importance to understand how muscle tissue is regenerated. So far, it has been known that the formation of muscle tissue with proper muscle function is favored by global, unified alignment. Using C2C12 mouse myoblasts as a model system, micropatterning[2−6] has been used to guide cell alignment, fusion, and striation, which facilitates the success of myotube formation.[4,5]

In recent years, cells on micropatterns were found with particular chiral mechanics.[7] When cultured on micropatterns, adherent cells[7,8] were reported with specific chirality in cell polarity,[7,9] cell−cell alignment[7,8] and multicellular organization.[7,10,11] C2C12 myoblasts were also found with chiral orientation on micropatterns,[8] especially on rigid substrate such as glass.[12] Remarkably, such chiral mechanics are associated with actomyosin activity. That is, chirality in cell migration was activated with accumulation of actomyosin stress fibers,[7,8] but suppressed or even reversed when actin was inhibited.[8] The importance of actomyosin activity inspired the development of a nanowire magnetoscope that discovered a new type of chiral force—torque with rotational bias—being exerted by cells.[13] Further analysis suggested that the generation of chiral torque is associated with an actin ring composed of two classes of actin filaments: transverse arc and dorsal stress fibers.[14,15] On the basis of such arrangement, cell chirality can be driven by a tangential shift of transverse arc accompanying with unidirectionally tilted dorsal fibers. Thus, as a mechanical behavior associated with actin cytoskeleton, cell's intrinsic chirality plays an essential role in guiding the

Special Issue: Biomaterials for Mechanobiology

Received: November 2, 2018
Accepted: May 20, 2019
Published: June 4, 2019

DOI: 10.1021/acsbiomaterials.8b01364
ACS Biomater. Sci. Eng. 2019, 5, 3944−3953

specific chiral orientation of myoblasts as well as the myotube formation.

Notably, culture density can serve as an active participant in regulating cell's mechanical behaviors. Culture density regulates cell shape and cytoskeletal contractility, which later controls the lineage commitment of human mesenchymal stem cells,[16,17] and promotes redifferentiation of dedifferentiated human chondrocytes.[18] More specifically, cell morphology and size can also be changed following a series of in vitro cultures.[19−21] Such a notion is correlated to the density-dependent changes in cell shape and microfilament organization.[22] Thus, the influence on actin cytoskeleton by cultures with different densities may also affect the expression of cell chirality.

In this report, we study the remnant effects on cell chirality by a series of subcultures with high/low density. C2C12 myoblasts were seeded with density at 2200 cells/cm^2 (low density) or 22 000 cells/cm^2 (high density) during each subculture. After a series of subcultures, we found that the cells with prior exposure to low-density culture exhibited a chiral orientation on micropatterned stripes on glass substrate but not on PDMS substrate. In contrast, high-density culture enabled a chiral rotation of single cells and an enhanced chiral orientation independent of substrate material. More importantly, comparing to the original cells without being subcultured with high/low density, we found that low-density culture disorganized the formation of actin ring in single cells. Moreover, using high-density culture supplemented with cytochalasin D (CD) or latrunculun A (LatA) that perturbs actin polymerization, the effect of low-density culture was recaptured, suggesting that the remnant effect on cell chirality by low-density culture might be comparable to an in vitro aging that causes a cumulative modification on actin cytoskeleton. Our result suggests that culture density serves as a "dose" that results in a "structural memory" on the cell chirality even after trypsin digestion and reseeding, providing a possible way to reconstitute the chiral morphology on different substrates.

MATERIALS AND METHODS

Micropatterning. Micropatterns of cell-adhering islands were fabricated by photolithography. For PDMS (Dow Corning) substrate, the elastomer precurser was mixed with cross-linker at 30 to 1 ratio. After evenly spreading on a cleaned glass and reflowing, the PDMS was cured by overnight baking at 70 °C, followed by plasma treatment (800 mTorr at 30W, 2 min) to activate the surface before the photolithography. For glass substrate, it was cleaned by piranha solution (sulfuric acid to hydrogen peroxide = 3:1) for an hour. Next, both glass and PDMS substrates were treated with hexamethyldislazane (HMDS, Sigma) coating in vapor phase for 5 min. Next, AZ5214 photoresist (PR, AZ Electronic Materials, Luxembourg) was spin-coated on the substrates at 3000 rpm and baked at 95 °C for 2 min. After UV exposure and development, they were coated with fibronectin solution (20 μg/mL, Life Technology) for an hour, followed by removing the remaining photoresist by 3 rinsing steps (5 min each) using absolute ethanol. Finally, the substrates were coated with 1% pluronic F127 for 50 min before cell seeding.

Cell Culture. Mouse myoblasts (C2C12, ATCC) were cultured in high glucose Dulbecco's modified Eagle's medium supplemented with 10% fetal bovine serum and 1% penicillin−streptomycin (Gibco) and kept in humidified incubator at 37 °C with 5% CO_2. Myoblasts were expanded at a plating density of 5000 cells/cm^2 until passage 8 (P8). From passage 9 (P9) to 13 (P13), we used seeding density of 2200 cells/cm^2 (low density) or 22,000 cells/cm^2 (high density), and the subcultures were repeated for every 2 days (passage +1 at each subculture). For drug treatment, culture medium was supplemented with actin inhibitor, CD in 500 nM, LatA in 500 nM, or ethylene glycol tetraacetic acid (EGTA) in 1 mM. To measure the cell size, we prestained 10% cells with CellTracker Green CMFDA Dye (2.5 μM, Life Technologies) before seeding.

Orientation Analysis of Fixed Cells on Micropatterned Stripes. We seeded P9 cells or P13 cells onto micropatterned stripes (width = 200 μm) on glass and PDMS substrate with a seeding density of 75,000 cells/cm^2. After 12 h of incubation, the cell nuclei were stained by treating with 4% paraformaldehyde (PFA) for 15 min, 0.1% Triton X-100 for 10 min, and DAPI (300 nM, Thermal Fisher) staining for 5 min. Fluorescence images were taken by Nikon Ti-E fluorescence microscope. We calculated cell orientation using the acute angle θ between the long axis of cell nucleus and the horizontal axis of the stripe boundary, as described previously[12] (MATLAB source code available at online repository: https://github.com/GiovannaHUANG/Outline-Etching-Cell-Chirality.git). In brief, the fluorescence-stained nucleus was initially separated based on Boolean addition of two binarized images using global and adaptive thresholds. Next, the overlapping nucleus contours in the binarized images of cells were segmented by iteratively etching the outlines of nuclei, which allows the acquisition of orientations of each individual cell. Finally, the orientation of the long axis was obtained by ellipse detection, which is defined positive when the acute angle θ is within $[0, 90]$ and negative when θ is within $[-90, 0]$. As such, the chirality can be determined based on the statistical difference between the percentages of cells with positive and negative orientation derived from cells on multiple stripes.

Fluorescent Staining of Actin and β-catenin. To stain the actin, cells were seeded on circular patterns with areas of 500 μm^2 or 2500 μm^2 using cell number to pattern number at 1:1 ratio. They were incubated in growth medium for 6 h. Before staining, cells were treated with 4% PFA for 15 min, 0.2% Triton X-100 for 10 min, Image-iT FX (Thermo Fisher Scientific) signal enhancer for 30 min, Rhodamine Phalloidin (1/40, Life Technology) for an hour, and DAPI (300 nM, Thermal Fisher Scientific) staining for 5 min. To simultaneously stain the β-catenin and actin, cells were treated by 4% PFA for 15 min, 0.2% Triton X-100 for 10 min, Image-iT FX (Thermo Fisher Scientific) signal enhancer for 30 min, β-catenin monoclonal antibody for 1 h (1/30, Life Technology), secondary goat antimouse IgG-Alexa Fluor 488 (1/250, Life Technology) for an hour, followed by Rhodamine Phalloidin (1/40, Life Technology) for an hour, and DAPI (300 nM, Thermal Fisher) staining for 5 min. The samples were then mounted with Fluoromount G (Electron Microscopy Sciences. Inc.) and imaged by inverted fluorescence microscopy.

Live Cell Rotation. For single cells on circular micropatterns, P9 or P13 C2C12 cells were seeded on circular patterns with areas of 500 μm^2 on glass, or 2,500 μm^2 on glass or PDMS using cell number to pattern number at 1:1 ratio. The live nucleus was stained with 2 μg/mL of bisBenzimide H 33342 trihydrochloride (Sigma-Aldrich) for 30 min. Live cells were imaged by Nikon Eclipse Ti-E microscope at every 10 min for 2 h on circular micropatterns. To measure the cell rotation, we used the long axis of individual nucleus as a reference, and the transient angular velocity of nucleus rotation was calculated based on the change of orientation angle divided by the time interval between two consecutive images. The transient angular velocity in anticlockwise (ACW) rotation was defined as positive (+), while in clockwise (CW) rotation was defined as negative (−). Afterward, the percentages of ACW or CW transient angular velocity of each cell within the observation duration were averaged among many cells. Next, the chirality was determined based on the statically significant difference between these two percentages using Student's t test.

Cell Aspect Ratio. Before seeding to micropatterned stripes, myoblasts stained with 2.5 μM of CellTracker Green CMFDA Dye for 30 min were mixed with other cells without staining in proportion of 1:10. After incubation for 12 h, the cells were fixed by 4% PFA and imaged. The aspect ratio was then measured by Nikon Element manual 5-point ellipse approximation. At least 100 samples were measured in each case.

DOI: 10.1021/acsbiomaterials.8b01364
ACS Biomater. Sci. Eng. 2019, 5, 3944−3953

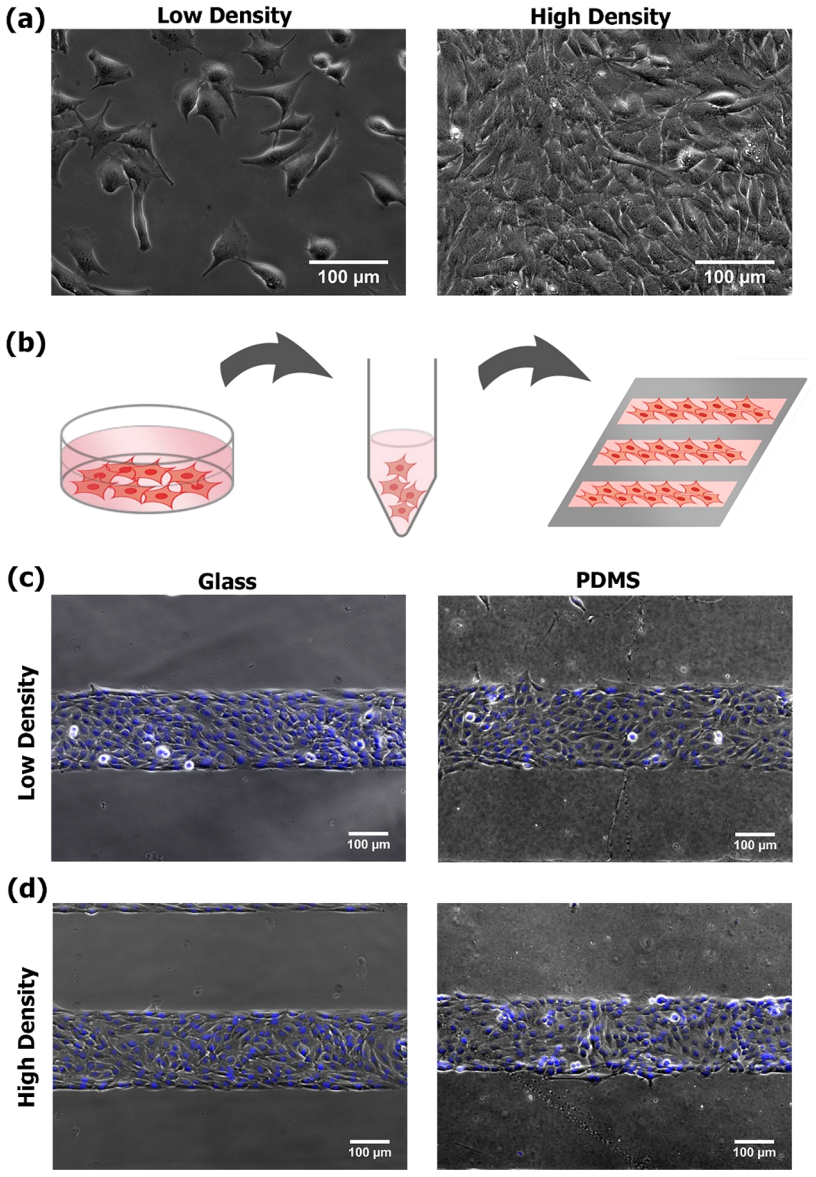

Figure 1. Cells seeding on micropatterned stripes after a series of subcultures with high/low cell density. (a) Phase contrast image of cultures with high and low cell density. (b) Schematics showing that, after a series of subcultures, cells were resuspended from the high-/low-density culture and reseeded onto the micropatterned stripes, where the gray regions are coated with cell-repellent pluronic and the pink regions are coated with cell-adherent fibronectin. (c, d) Phase contrast images of cells on micropatterned stripes on glass or PDMS substrate with DAPI-stained nuclei using cells after (c) low- or (d) high-density cultures.

Intercellular Alignment. The measurement of intercellular alignment was carried out based on the orientation angle θ of each cell obtained previously. Acute angle difference, $|\Delta\theta|$, was calculated by each cell with its neighboring cells with cell−cell distance less than 55 μm (120 pixels).

Statistical Analysis. Student's t test was applied to compare the percentage of cells with positive and negative orientation, and the percentage of transient angular velocity of each cell in CW and ACW direction. The confidence level was set to be 0.05 for all statistical tests. The statistical significance was symbolized by ns ($p > 0.05$), * ($p \leq 0.05$), ** ($p \leq 0.01$), *** ($p \leq 0.001$), or **** ($p \leq 0.0001$).

RESULTS

Chiral Orientation of Cells Reseeded After Low- or High-Density Subcultures. We first investigated the chiral behavior of cells reseeded from a series of subcultures with low or high cell density. Long stripes on glass or PDMS substrate were used to reveal the chiral orientation. It is based on our previous finding that cells can accumulate their actomyosin stress fibers when encountering the interface between cell-adherent and cell-repellent substrates, which allows cells to migrate and orient with LR bias, or chirality.[7] Thus, the requirement of actomyosin stress fibers suggested a possible dependence of chiral mechanics on substrate stiffness, as discussed previously.[12] C2C12 myoblasts were seeded with low (seeding density at 2200 cells/cm^2 at each passage) or high cell density (seeding density at 22 000 cells/cm^2 at each passage) from P9 to P12 (Figure 1a). At P9 and P13, cells were seeded onto alternating micropatterned stripes with cell-adherent (fibronectin) and cell-repellent (pluronic) coatings on glass or PDMS substrate (Figure 1b). After 12 h of incubation, cells were fixed and stained, allowing the analysis of cell orientation (Figure 1c, d).

Fluorescence images of cell nuclei were used to analyze cell orientation (Figure 2a), which is defined as the acute angle

DOI: 10.1021/acsbiomaterials.8b01364
ACS Biomater. Sci. Eng. 2019, 5, 3944−3953

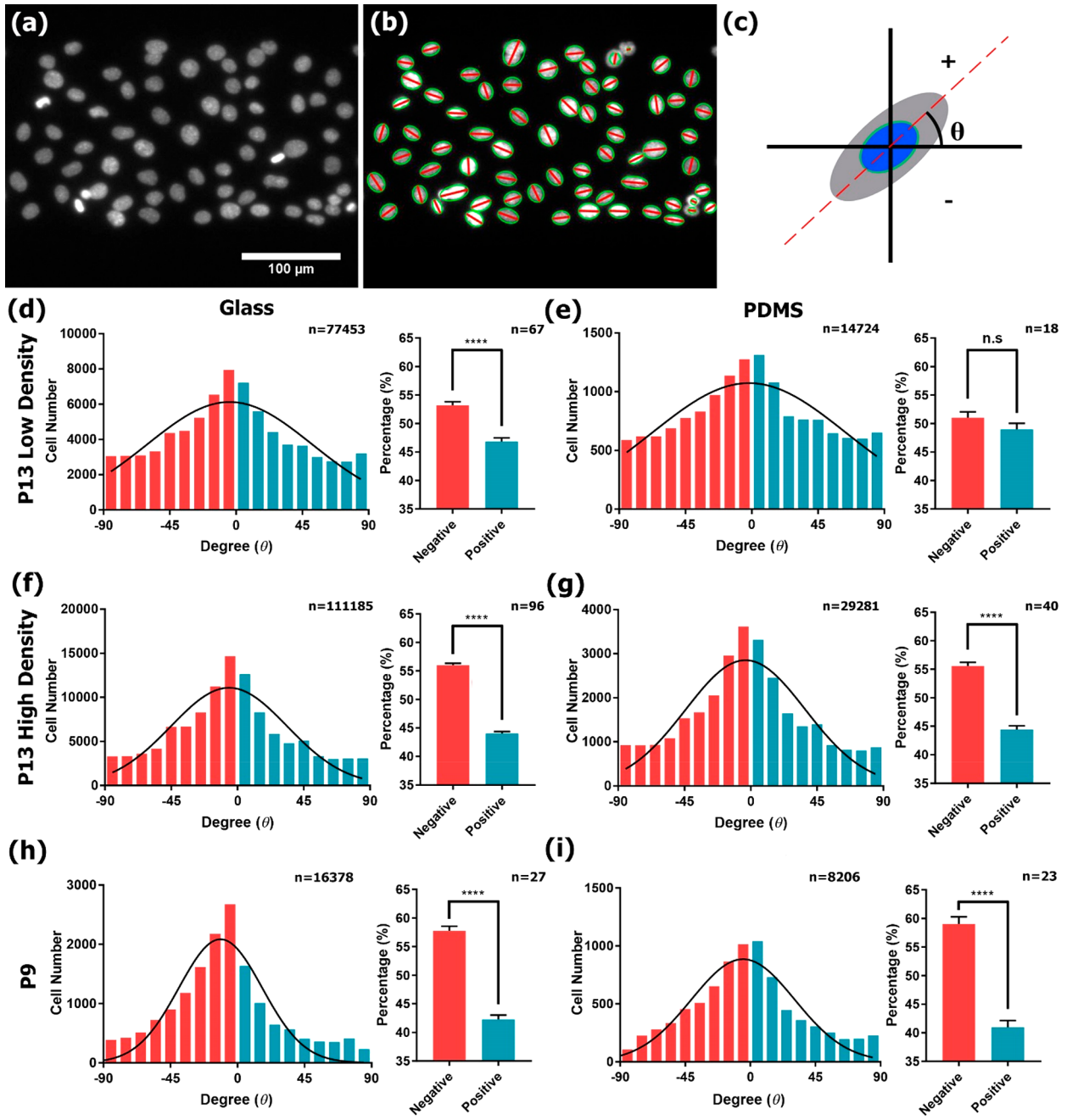

Figure 2. Chiral orientation of cells on micropatterned stripes. (a) Fluorescent microscopy images of DAPI-stained cell nuclei. (b, c) Orientation analysis based on the long axis of nuclei (b, red) relative to the horizontal stripe boundary, where the orientation angle θ is defined positive when the acute angle θ is within [0, 90] and negative when θ is within [−90, 0] (c). (d–i) Histogram of cell orientation on (d, f, h) glass or (e, g, i) PDMS substrate using (h, i) P9 cells or P13 cells from a series of subcultures with (d, e) low or (f, g) high cell density.

difference between the long axis of cell nucleus (Figure 2b) and horizontal stripe boundary (Figure 2c). We found that, for cells after low-density cultures and reseeded on micropatterned stripes on glass, the percentage of cells with negative orientation was 53 ± 0.64%, and the chirality was revealed by the significant difference between the percentage of cells with positive and negative orientation (Figure 2d). As a comparison, when cultured on micropatterned stripes on PDMS, the negative percentage was 51 ± 1.03%, and the chirality was insignificant (Figure 2e), suggesting a reduction of cell chirality dependent on substrate material. In contrast, for cells after high-density culture, the percentage of cells with negative orientation on glass and PDMS substrate were both above 55% with significant chirality (Figure 2f, g), which is consistent with the P9 cells (Figure 2h, i). Together, it suggests that cells isolated from cultures with low density exhibited attenuated chirality, making it dependent on substrate material.

Cell Aspect Ratio. When cultured on glass and PDMS substrate, cell may respond to substrate stiffness by regulating its contractility and polarization, leading to a change of cell's aspect ratio.[23] To measure it, 10% of cells were stained by CellTracker Green CMFDA Dye before seeded onto micropatterned stripes on glass or PDMS substrate, and the aspect ratio was measured by 5-point ellipse approximation (Figure

DOI: 10.1021/acsbiomaterials.8b01364
ACS Biomater. Sci. Eng. 2019, 5, 3944–3953

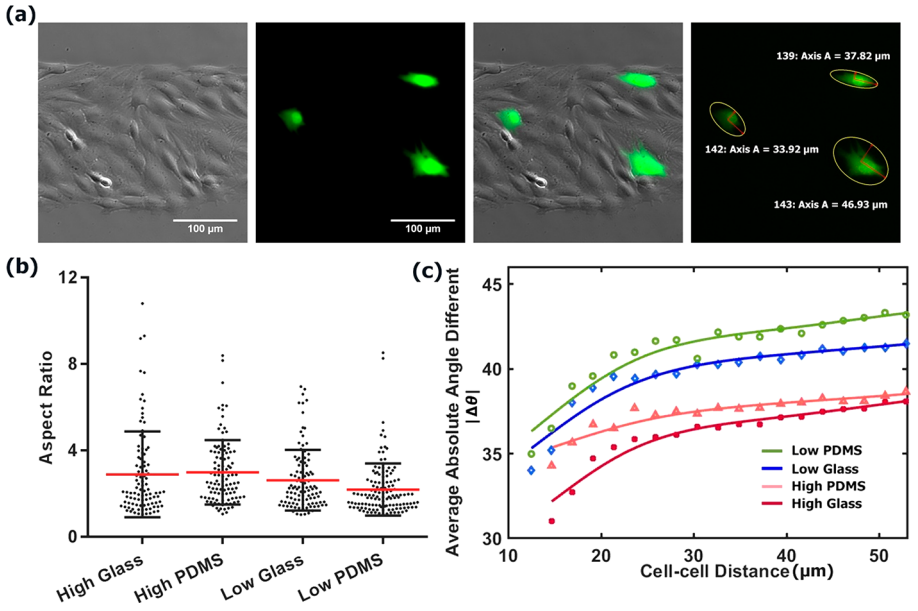

Figure 3. Cell aspect ratio and intercellular alignment when cultured on micropatterned stripes on different substrates. (a) The measurement of cell aspect ratio on stripes. Phase-contrast image of all cells (leftmost) and fluorescence image of 10% cells stained with cell tracker (second left) are merged (second right), which allows the measurement of aspect ratio by Nikon Element manual 5-point ellipse approximation (rightmost). (b) The aspect ratio of cells on stripes on glass substrate using cells after high-density (High Glass) or low-density culture (Low Glass), or on PDMS substrate using cells after high-density (High PDMS) or low-density culture (Low PDMS). (c) The intercellular alignment against cell−cell distance measured by the absolute angle difference $|\Delta\theta|$ between cells and their neighbors using cells after high-density (High Glass) or low-density culture (Low Glass), or on PDMS substrate using cells after high-density (High PDMS) or low-density culture (Low PDMS).

3a). Interestingly, prior exposure to high-density culture increased the cell's aspect ratio after seeding on either glass or PDMS substrate (3.02 ± 2 on glass and 2.99 ± 1.48 on PDMS substrates, mean ± SD, Figure 3b). In contrast, for cells after low-density culture, the aspect ratio was reduced on glass substrate (2.62 ± 1.4, Figure 3b) and further reduced on PDMS substrate (2.19 ± 1.2, Figure 3b). This result indicates that prior exposure to high-density subcultures maintained cell contractility, making it independent of substrate stiffness. On the other hand, cell contractility was reduced after low-density culture and became dependent on substrate stiffness. Thus, our results suggest that low-density culture makes cells less contractile and sensible to the substrate stiffness.

To further elucidate the difference of cell aspect ratio, we measured the intercellular alignment in the formation of chiral orientation on micropatterned stripes. Cell−cell adhesion is suggested as a mediator to propagate and amplify the chiral mechanics of cells.[24] Therefore, cells with higher aspect ratio, i.e., more elongated cells, may demonstrate enhanced intercellular alignment to amplify the expression of chiral orientation. We used absolute, acute angle difference $|\Delta\theta|$ between one cell and its neighbors as a quantitative measure of intercellular alignment, as reported previously.[25] After averaging the $|\Delta\theta|$ of pairs of cells with different cell−cell distance, we found that $|\Delta\theta|$ was reduced with shorter cell−cell distance, suggesting a better intercellular alignment between cells and their nearest neighbors (Figure 3c). More importantly, the $|\Delta\theta|$ of cells after low-density culture was always greater than the $|\Delta\theta|$ of cells after high-density culture, and was even greater on PDMS substrate compared to that on glass substrate. Such increased $|\Delta\theta|$ indicates less intercellular alignment on PDMS substrate when using cells after low-density culture, providing further evidence that the aspect ratio was indeed reduced, leading to an ineffective intercellular alignment which prohibits the propagation and amplification of chiral orientation.

Chirality of Single Cell After Reseeding. We next investigated the cell chirality of single cells after the high- or low-density cultures. Although the amplification of chiral orientation became ineffective because of the decreased aspect ratio and impaired intercellular alignment after low-density culture, it remains unclear whether the chiral mechanics of single cells were truly affected. That is, individual cells might still exhibit similar chiral mechanics after high- or low-density cultures, but the different, impaired intercellular alignment due to low-density culture makes the propagation of chiral orientation more difficult, leading to different chiral orientation. To investigate it, we measured the nucleus rotation of single cells after reseeding P13 cells onto circular micropatterns with size of 500 μm^2, which was designed based on the nature spreading area of cells in either low- (726.62 ± 52.42 μm^2, Figure S1) or high-density culture (536.97 ± 40.94 μm^2, Figure S1). After incubation for 3 h, the nucleus was stained as aforementioned for measurement of cell rotation. We found that P13 cells after low-density culture exhibited a slight, insignificant CW-biased rotation (Figure 4a). In contrast, the CW rotational bias was much more significant for P13 cells after high-density culture (Figure 4b). Thus, the low-density culture not only reduced the cell aspect ratio and impaired intercellular alignment but also reduced the chiral mechanics of single cells.

Likewise, such down-regulation of cell aspect ratio (Figure 3b), intercellular alignment (Figure 3c), and chiral rotation of single cells (Figure 4a), should be associated with the overall reduction of cell contractility and F-actin. We next visualized the actin filament through fluorescence staining. On circular pattern with area of 500 μm^2, we observed a strong expression of ventral actin fibers (Figure 4d), and such filament was more

DOI: 10.1021/acsbiomaterials.8b01364
ACS Biomater. Sci. Eng. 2019, 5, 3944−3953

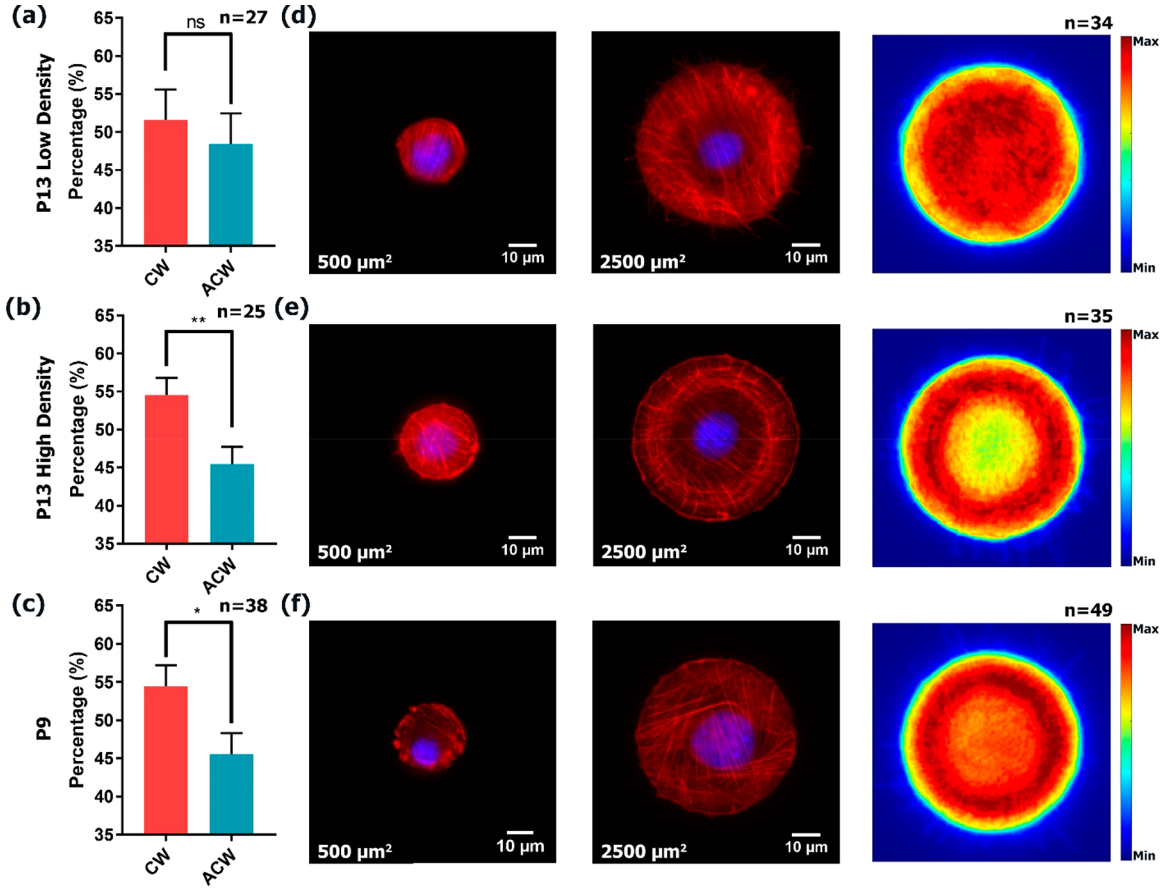

Figure 4. Cell chirality on micropatterned circular islands. (a–c) The percentage of CW/ACW rotation of each P13 cell after subcultures with (a) low or (b) high cell density or (c) P9 cells. (d–f) Actin cytoskeleton of cells on 500 μm^2 (left) and 2500 μm^2 (middle) circular islands, and heat map (right) of actin distribution by stacking images of actin on 2500 μm^2 circular islands using cells after subcultures with (d) low or (e) high cell density or (f) P9 cells.

distinct in P13 cells after high-density culture (Figure 4e). To better illustrate the distribution of actin fibers, we used circular pattern with area of 2500 μm^2, which allows myoblasts to spread fully. Interestingly, comparing the actin distribution, P13 cells after high-density culture showed more distinct distribution of dorsal stress fibers and transverse arc (Figure 4e). After stacking the images, a clear actin ring was well arranged in P13 cells after high-density culture on glass substrate (Figure 4e) or PDMS substrate (Figure S2b). In contrast, for P13 cells after low-density culture, the actin filaments were more disorganized and evenly distributed on both substrates (Figure 4d and Figure S2a). Thus, our results suggest that the reduced chirality of cells after low-density culture is associated with the disorganized actin ring resulted from the low-density culture.

Note that the chiral rotation and the actin ring formation of high-density P13 cells are similar with that of P9 cells (Figure 4c, f). In contrast, low-density P13 cells expressed reduced chirality in cell orientation (Figure 2d, e), rotation (Figure 4a), and disorganized actin ring (Figure 4d). These results suggest that exposure to low-density cultures from P9 to P13 may attenuate the actin ring or even disorganize the actin configuration. Previously we found that the chiral rotation and the actin ring appear preferably in single cells with rounded shapes.[13] For noncircular, elongated cells, the actin ring is rearranged into linear actin fibers, and the chiral mechanics disappear.[13] Thus, the cells cultured in low density may be allowed to spread more spaciously that reinforces the irregularity of cell shape, which may down-regulate the F-actin and formation of actin ring. Of note, subculture is a common in vitro aging process. Increasing passage number was found to affect the organization of F-actin and cell contraction,[26] and alter cell morphology and size.[19−21] Thus, the series of subcultures from P9 to P13 could be similar to the in vitro aging process by which high/low-density culture can alter the actin cytoskeleton, allowing cells with a cumulative, embedded structural "memory" remnant on cell chirality after trypsin digestion and cell reseeding.

To confirm that the modification of actin during the aging process from P9 to P13 is the key to such memory, we applied CD, which binds to the growing ends of actin filament and inhibits the actin polymerization,[27] or LatA, which inhibits actin polymerization by binding with G-actin sequestering monomeric actin.[28] Such treatment in high-density culture resembles the down-regulation of F-actin and actin ring after low-density culture. After the series of high-density subcultures with CD or LatA, P13 cells were reseeded on micropatterns, and the medium was switched back to normal medium. With the prior inhibition of actin polymerization by CD, we found that cells exhibited a reversed, positive bias in cell orientation on glass (Figure 5a) and neutral, unbiased orientation on PDMS substrate (Figure 5b). For actin polymerization inhibition by LatA during subcultures, the cell showed positive bias on both glass and PDMS substrates (Figure 5c, d). The

DOI: 10.1021/acsbiomaterials.8b01364
ACS Biomater. Sci. Eng. 2019, 5, 3944−3953

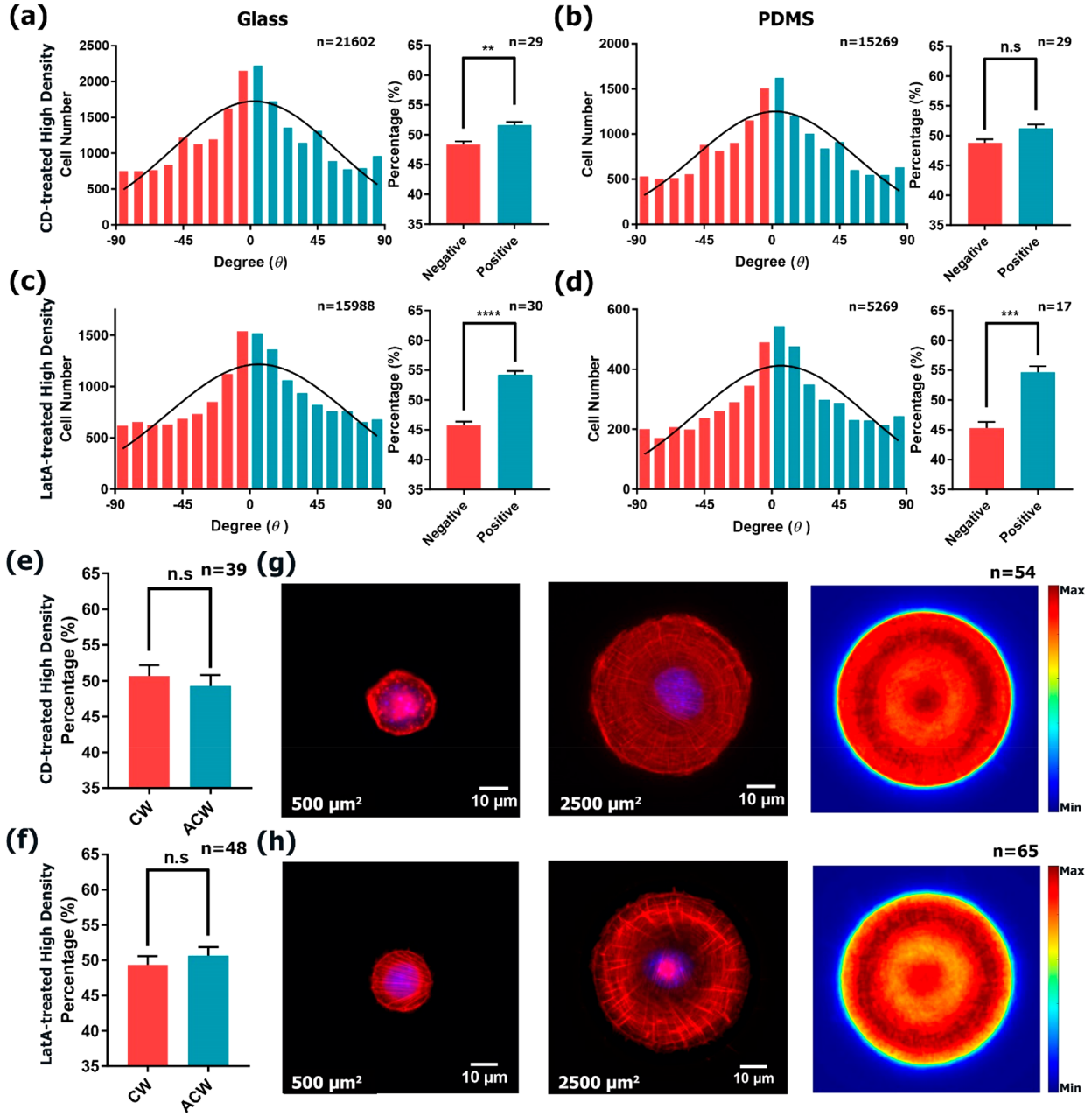

Figure 5. Chirality of cells after high-density cultures with cytochalasin D (CD) and latrunculin A (LatA). (a, b) Histogram of cell orientation on (a) glass or (b) PDMS substrate after high-density cultures with CD. (c, d) Histogram of cell orientation on (c) glass or (d) PDMS substrate after high-density cultures with LatA. (e) The percentage of CW/ACW rotation of each cell after high-density cultures with CD. (f) The percentage of CW/ACW rotation of each cell after high-density cultures with LatA. (g) Actin cytoskeleton of cells on 500 μm^2 (left), 2500 μm^2 (middle) circular islands, and heat map (right) of actin distribution by stacking images of actin on 2500 μm^2 circular islands using cells after high-density cultures with CD. (h) Actin cytoskeleton of cells on 500 μm^2 (left), 2500 μm^2 (middle) circular islands, and heat map (right) of actin distribution by stacking images of actin on 2500 μm^2 circular islands using cells after high-density culture with LatA.

chiral rotation became neutral as well (Figure 5e, f). Moreover, the actin ring appeared to be disorganized (Figure 5g, h), which was similar to that in low-density P13 cells. Thus, we conclude that the loss of cell chirality in rotation and actin ring in low-density culture is associated with modified actin cytoskeleton which creates cumulative, embedded structural "memory" remnant on cell chirality.

DISCUSSION

Such a remnant effect may be comparable to other types of mechanical memory. Recently, a profound experiment demonstrated that, with appropriate mechanical cues such as stiffness, muscle stem cells showed self-renewal in culture, and pertained its regenerative properties after transplantation.[29] This implies that cells can be conditioned with "memory" of the past mechanical environments, allowing a long-term influence in cell's fate such as osteogenic differentiation.[30] In addition, cell alignment through nanofabricated topography was reported with the ability to maintain its alignment even after the cell monolayers were detached or removed from the nanotopographical cues.[31] Together, those reports collectively suggest that actin structure can be modified as the structural

DOI: 10.1021/acsbiomaterials.8b01364
ACS Biomater. Sci. Eng. 2019, 5, 3944−3953

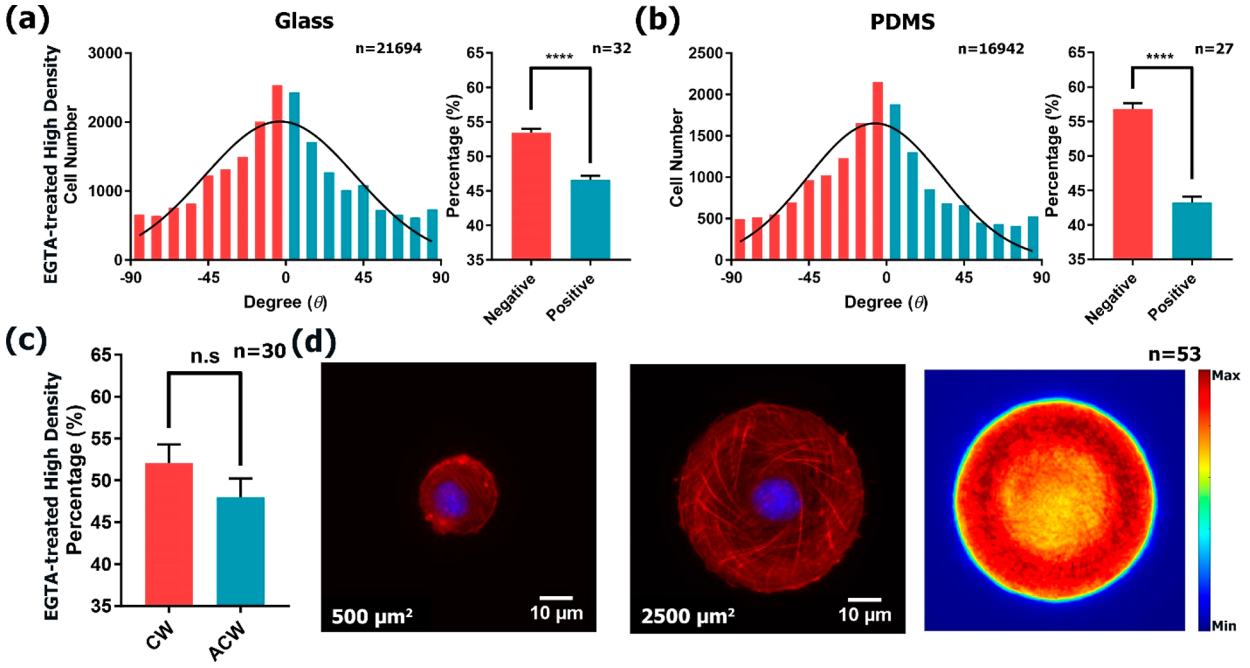

Figure 6. Chirality of cell after high-density cultures with ethylene glycol tetraacetic acid (EGTA). (a, b) Histogram of cell orientation on (a) glass or (b) PDMS substrate. (c) The percentage of CW/ACW rotation of each cell after high-density cultures with EGTA. (d) Actin cytoskeleton of cells on 500 μm^2(left), 2500 μm^2 (middle) circular islands, and heat map (right) of actin distribution by stacking images of actin on 2500 μm^2 circular islands using cells after high-density culture with EGTA.

memory, enabling the exhibition of a particular cell's behavior even after the microenvironment is changed.

Note that absence of cell−cell contact is the primary difference between high-density and low-density culture, as stained by β-catenin (Figure S3a-c). To test the effect, we applied ethylene glycol tetraacetic acid (EGTA), which disrupts adheren junctions[24] during the series of subcultures with high density (Figure S 3d). However, the chiral orientation was observed on both glass and PDMS substrate (Figure 6a-b). While the chirality of cell rotation was reduced (Figure 6c), the actin ring was undamaged (Figure 6d) and similar to that of P9 cells (Figure 4f), suggesting that cell−cell contact is not the reason for such modification of actin cytoskeleton and chiral mechanics. Instead, we believe that the modification of actin is a result of the free space in low-density culture, which allows cells to stretch, deform, leading to irregular and noncircular cell shape. This notion is consistent with our previous finding that elongated cell shape would disrupt the formation of actin ring, making the chiral behavior not observed in regular culture.[13] Thus, although low-density culture has been suggested to maintain cell phenotype since it avoids the contact inhibition and prevent cell differentiation, our results indicate that the low-density culture may, on the other hand, attenuate the chiral behavior of cells. Thus, balance needs to be considered when aiming to reproduce and guide the chiral mechanics in an engineering context such as regeneration of various tissue/organ with specific LR alignment and architecture.

Interestingly, after treatment of CD or LatA, cells exhibited unbiased cell rotation and a positive chiral orientation (Figure 5). Such reversal of chiral orientation by inhibition of actin polymerization is consistent with pervious findings.[8,12,32] However, cells after low-density culture exhibited unbiased cell rotation but the orientation remained negative. Such difference suggests that inhibition of actin polymerization can only partially recapture the remnant effects of low-density culture. Other factors such as α-actinin that cross-links radial actin fibers might play a role in reversing the cell chirality, as suggested by other reports.[32,33] Further investigation on micropatterns that forces cells to form arbitrary and irregular shapes in long-term cultivation may be used to further investigate the remnant remolding of actin filament by low-density culture. Our findings of culture density call for further investigation of the structural memory in cytoskeletal chirality.

CONCLUSIONS

Regeneration of skeletal muscle requires specific guidance of myotube formation, which is essential for proper muscle function and body movement. The alignment of myoblasts may involve cell's intrinsic chirality, allowing the expression of chiral orientation during myogenesis. However, understanding of such chiral morphogenesis remains limited. In this work, we report remnant effects of culture density after a series of subcultures and reseeding on micropatterns. We found that the prior exposure to low-density culture attenuated cell chirality. In contrast, high-density culture enabled cells to express chiral orientation and rotation. More importantly, such change was associated with the formation of actin ring, which was disorganized in cells experiencing in low-density culture, suggesting that the series of subcultures from P9 to P13 with low density could be an in vitro aging process that modified actin filament as a structural "memory," resulting in a remnant effects on the cell chirality. Together, it provides a mechanistic insight of how cytoskeletal structure can "memorize" the previous experience, raising a new perspective for rebuilding artificial tissue constructs with inherent LR asymmetry in the future.

DOI: 10.1021/acsbiomaterials.8b01364
ACS Biomater. Sci. Eng. 2019, 5, 3944−3953

■ ASSOCIATED CONTENT

Supporting Information

The Supporting Information is available free of charge on the ACS Publications website at DOI: 10.1021/acsbiomaterials.8b01364.

Cell size measurement, actin ring on PDMS substrate, and actin and β-catenin staining of cells in low- or high-density culture (PDF)

■ AUTHOR INFORMATION

Corresponding Author

*Email: thchen@cityu.edu.hk.

ORCID

Ting-Hsuan Chen: 0000-0003-4517-7750

Notes

The authors declare no competing financial interest.

■ ACKNOWLEDGMENTS

We are pleased to acknowledge the technical assistance of image processing by Ka Yu Fung and the funding support from the Early Career Scheme (project 21214815) and General Research Fund (projects 11277516 and 11217217) of the Hong Kong Research Grant Council, the Science Technology and Innovation Committee of Shenzhen Municipality (grant JCYJ20170307091338607), and internal grants from City University of Hong Kong (9667161 and 6000632).

■ REFERENCES

(1) Ostrovidov, S.; Hosseini, V.; Ahadian, S.; Fujie, T.; Parthiban, S. P.; Ramalingam, M.; Bae, H.; Kaji, H.; Khademhosseini, A. Skeletal Muscle Tissue Engineering: Methods to Form Skeletal Myotubes and Their Applications. *Tissue Eng., Part B* **2014**, *20* (5), 403−436.

(2) Bajaj, P.; Reddy, B.; Millet, L.; Wei, C. N.; Zorlutuna, P.; Bao, G.; Bashir, R. Patterning the Differentiation of C2C12 Skeletal Myoblasts. *Integr Biol-Uk* **2011**, *3* (9), 897−909.

(3) Junkin, M.; Leung, S. L.; Whitman, S.; Gregorio, C. C.; Wong, P. K. Cellular Self-Organization by Autocatalytic Alignment Feedback. *J. Cell Sci.* **2011**, *124* (24), 4213−4220.

(4) Engler, A. J.; Griffin, M. A.; Sen, S.; Bönnemann, C. G.; Sweeney, H. L.; Discher, D. E. Myotubes Differentiate Optimally on Substrates with Tissue-like Stiffness: Pathological Implications for Soft or Stiff Microenvironments. *J. Cell Biol.* **2004**, *166* (6), 877−887.

(5) Ren, K.; Crouzier, T.; Roy, C.; Picart, C. Polyelectrolyte Multilayer Films of Controlled Stiffness Modulate Myoblast Cell Differentiation. *Adv. Funct. Mater.* **2008**, *18* (9), 1378−1389.

(6) Sun, Y.; Duffy, R.; Lee, A.; Feinberg, A. W. Optimizing the Structure and Contractility of Engineered Skeletal Muscle Thin Films. *Acta Biomater.* **2013**, *9* (8), 7885−7894.

(7) Chen, T.-H.; Hsu, J. J.; Zhao, X.; Guo, C.; Wong, M. N.; Huang, Y.; Li, Z.; Garfinkel, A.; Ho, C.-M.; Tintut, Y.; Demer, L. L. Left-Right Symmetry Breaking in Tissue Morphogenesis via Cytoskeletal Mechanics. *Circ. Res.* **2012**, *110* (4), 551−559.

(8) Wan, L. Q.; Ronaldson, K.; Park, M.; Taylor, G.; Zhang, Y.; Gimble, J. M.; Vunjak-Novakovic, G. Micropatterned Mammalian Cells Exhibit Phenotype-Specific Left-Right Asymmetry. *Proc. Natl. Acad. Sci. U. S. A.* **2011**, *108* (30), 12295−12300.

(9) Xu, J.; Van Keymeulen, A.; Wakida, N. M.; Carlton, P.; Berns, M. W.; Bourne, H. R. Polarity Reveals Intrinsic Cell Chirality. *Proc. Natl. Acad. Sci. U. S. A.* **2007**, *104* (22), 9296−9300.

(10) Fan, J.; Ray, P.; Lu, Y. W.; Kaur, G.; Schwarz, J. J.; Wan, L. Q. Cell Chirality Regulates Intercellular Junctions and Endothelial Permeability. *Sci. Adv.* **2018**, *4* (10), eaat2111.

(11) Ray, P.; Chin, A. S.; Worley, K. E.; Fan, J.; Kaur, G.; Wu, M.; Wan, L. Q. Intrinsic Cellular Chirality Regulates Left-Right Symmetry Breaking During Cardiac Looping. *Proc. Natl. Acad. Sci. U. S. A.* **2018**, *115* (50), E11568−E11577.

(12) Zhu, N. H.; Kwong, H. K.; Bao, Y.; Chen, T. H. Chiral Orientation of Skeletal Muscle Cells Requires Rigid Substrate. *Micromachines-Basel* **2017**, *8* (6), 181.

(13) Liu, W.; Bao, Y.; Lam, M. L.; Xu, T.; Xie, K.; Man, H. S.; Chan, E. Y.; Zhu, N. H.; Lam, R. H. W.; Chen, T. H. Nanowire Magnetoscope Reveals a Cellular Torque with Left-Right Bias. *ACS Nano* **2016**, *10* (8), 7409−7417.

(14) Hotulainen, P.; Lappalainen, P. Stress Fibers Are Generated by Two Distinct Actin Assembly Mechanisms in Motile Cells. *J. Cell Biol.* **2006**, *173* (3), 383−394.

(15) Tojkander, S.; Gateva, G.; Lappalainen, P. Actin Stress Fibers - Assembly, Dynamics and Biological Roles. *J. Cell Sci.* **2012**, *125* (8), 1855−1864.

(16) McBeath, R.; Pirone, D. M.; Nelson, C. M.; Bhadriraju, K.; Chen, C. S. Cell Shape, Cytoskeletal Tension, and RhoA Regulate Stem Cell Lineage Commitment. *Dev. Cell* **2004**, *6* (4), 483−495.

(17) Ye, K.; Cao, L. P.; Li, S. Y.; Yu, L.; Ding, J. Interplay of Matrix Stiffness and Cell-Cell Contact in Regulating Differentiation of Stem Cells. *ACS Appl. Mater. Interfaces* **2016**, *8* (34), 21903−21913.

(18) Schulze-Tanzil, G.; de Souza, P.; Castrejon, H. V.; John, T.; Merker, H. J.; Scheid, A.; Shakibaei, M. Redifferentiation of Dedifferentiated Human Chondrocytes in High-density Cultures. *Cell Tissue Res.* **2002**, *308* (3), 371−379.

(19) Gu, Y.; Li, T.; Ding, Y.; Sun, L.; Tu, T.; Zhu, W.; Hu, J.; Sun, X. Changes in Mesenchymal Stem Cells Following Long-Term Culture In Vitro. *Mol. Med. Rep.* **2016**, *13* (6), 5207−5215.

(20) Yang, Y.-H. K.; Ogando, C. R.; Wang See, C.; Chang, T.-Y.; Barabino, G. A. Changes in Phenotype and Differentiation Potential of Human Mesenchymal Stem Cells Aging In Vitro. *Stem Cell Res. Ther.* **2018**, *9* (1), 131.

(21) Sokolov, I.; Guz, N. V.; Iyer, S.; Hewitt, A.; Sokolov, N. A.; Erlichman, J. S.; Woodworth, C. D. Recovery of Aging-Related Size Increase of Skin Epithelial Cells: In Vivo Mouse and In Vitro Human Study. *PLoS One* **2015**, *10* (3), No. e0122774.

(22) Egan, J. J.; Gronowicz, G.; Rodan, G. A. Cell Density-Dependent Decrease in Cytoskeletal Actin and Myosin in Cultured Osteoblastic Cells - Correlation with Cyclic-Amp Changes. *J. Cell. Biochem.* **1991**, *45* (1), 93−100.

(23) Prager-Khoutorsky, M.; Lichtenstein, A.; Krishnan, R.; Rajendran, K.; Mayo, A.; Kam, Z.; Geiger, B.; Bershadsky, A. D. Fibroblast Polarization is a Matrix-Rigidity-Dependent Process Controlled by Focal Adhesion Mechanosensing. *Nat. Cell Biol.* **2011**, *13* (12), 1457−1465.

(24) Worley, K. E.; Shieh, D.; Wan, L. Q. Inhibition of Cell-cell Adhesion Impairs Directional Epithelial Migration on Micropatterned Surfaces. *Integr Biol-Uk* **2015**, *7* (5), 580−590.

(25) Huang, Y. Z.; Bao, Y. Y.; Kwong, H. K.; Chen, T. H.; Lam, M. L. Outline-Etching Image Segmentation Reveals Enhanced Cell Chirality Through Intercellular Alignment. *Biotechnol. Bioeng.* **2018**, *115* (10), 2595−2603.

(26) Gibson, J. M.; Milam, S. B.; Klebe, R. J. Late Passage Cells Display an Increase in Contractile Behavior. *Mech. Ageing Dev.* **1989**, *48* (2), 101−110.

(27) Casella, J. F.; Flanagan, M. D.; Lin, S. Cytochalasin-D Inhibits Actin Polymerization and Induces Depolymerization of Actin-Filaments Formed during Platelet Shape Change. *Nature* **1981**, *293* (5830), 302−305.

(28) Yarmola, E. G.; Somasundaram, T.; Boring, T. A.; Spector, I.; Bubb, M. R. Actin-Latrunculin A Structure and Function - Differential Modulation of Actin-Binding Protein Function by Latrunculin A. *J. Biol. Chem.* **2000**, *275* (36), 28120−28127.

(29) Gilbert, P. M.; Havenstrite, K. L.; Magnusson, K. E. G.; Sacco, A.; Leonardi, N. A.; Kraft, P.; Nguyen, N. K.; Thrun, S.; Lutolf, M. P.; Blau, H. M. Substrate Elasticity Regulates Skeletal Muscle Stem Cell Self-Renewal in Culture. *Science* **2010**, *329* (5995), 1078−1081.

DOI: 10.1021/acsbiomaterials.8b01364
ACS Biomater. Sci. Eng. 2019, 5, 3944−3953

(30) Yang, C.; Tibbitt, M. W.; Basta, L.; Anseth, K. S. Mechanical Memory and Dosing Influence Stem Cell Fate. *Nat. Mater.* **2014**, *13* (6), 645−652.
(31) Jiao, A.; Trosper, N. E.; Yang, H. S.; Kim, J.; Tsui, J. H.; Frankel, S. D.; Murry, C. E.; Kim, D. H. Thermoresponsive Nanofabricated Substratum for the Engineering of Three-Dimensional Tissues with Layer-by-Layer Architectural Control. *ACS Nano* **2014**, *8* (5), 4430−4439.
(32) Chin, A. S.; Worley, K. E.; Ray, P.; Kaur, G.; Fan, J.; Wan, L. Q. Epithelial Cell Chirality Revealed by Three-Dimensional Spontaneous Rotation. *Proc. Natl. Acad. Sci. U. S. A.* **2018**, *115* (48), 12188−12193.
(33) Tee, Y. H.; Shemesh, T.; Thiagarajan, V.; Hariadi, R. F.; Anderson, K. L.; Page, C.; Volkmann, N.; Hanein, D.; Sivaramakrishnan, S.; Kozlov, M. M.; Bershadsky, A. D. Cellular Chirality Arising from the Self-Organization of the Actin Cytoskeleton. *Nat. Cell Biol.* **2015**, *17* (4), 445−457.

DOI: 10.1021/acsbiomaterials.8b01364
ACS Biomater. Sci. Eng. 2019, 5, 3944−3953